

π-Extended Porphyrins

N-Annulated Perylene-Substituted and Fused Porphyrin Dimers with Intense Near-Infrared One-Photon and Two-Photon Absorption

Jie Luo,^[a] Sangsu Lee,^[b] Minjung Son,^[b] Bin Zheng,^[c] Kuo-Wei Huang,^[c] Qingbiao Qi,^[d] Wangdong Zeng,^[d] Gongqiang Li,^[a] Dongho Kim,^{*[b]} and Jishan Wu^{*[a, d]}

Abstract: Fusion of two *N*-annulated perylene (NP) units with a fused porphyrin dimer along the S_0 – S_1 electronic transition moment axis has resulted in new near-infrared (NIR) dyes **1a**/**1b** with very intense absorption ($\epsilon > 1.3 \times 10^5 \text{ M}^{-1} \text{ cm}^{-1}$) beyond 1250 nm. Both compounds displayed moderate NIR fluorescence with fluorescence quantum yields of 4.4×10^{-6} and 6.0×10^{-6} for **1a** and **1b**, respectively. The NP-substituted porphyrin dimers **2a**/**2b** have also been obtained by controlled oxidative coupling and cyclodehydrogenation, and they showed superimposed absorptions of

the fused porphyrin dimer and the NP chromophore. The excited-state dynamics of all of these compounds have been studied by femtosecond transient absorption measurements, which revealed porphyrin dimer-like behaviour. These new chromophores also exhibited good nonlinear optical susceptibility with large two-photon absorption cross-sections in the NIR region due to extended π -conjugation. Time-dependent density functional theory calculations have been performed to aid our understanding of their electronic structures and absorption spectra.

Introduction

Porphyrins and π -extended porphyrins have been extensively studied for applications in organic photovoltaics,^[1] molecular electronic materials,^[2] nonlinear optics,^[3] sensors,^[4] and so on. In particular, their rigid planar structures make them ideal candidates for third-order nonlinear optical (NLO) studies, such as two-photon absorption (TPA).^[5] Considerable efforts have been devoted to expansion of their π -electronic frameworks, as this would give rise to red-shifted one-photon absorption (OPA) and enhanced TPA cross-sections. Various strategies have been attempted, including the introduction of ethynylene^[6] or vinyl-

ene^[7] π -conjugated spacers, fusion of additional aromatic units,^[8] synthesis of longer *meso*–*meso*-linked porphyrin arrays,^[9] design of self-assembled porphyrin systems,^[10] development of expanded porphyrins,^[11] and so on. Among them, fused porphyrin tapes with triple covalent linkages at all three *meso*–*meso*, β – β , and β' – β' positions (Figure 1) have been demonstrated to be interesting chromophores by virtue of their strong near-infrared (NIR) absorption and large TPA cross-sections.^[12] Fusion of one or more polycyclic aromatic hydrocarbon (PAH) units, such as benzene, naphthalene, anthracene, azulene, or pyrene, at the periphery of porphyrins is another efficient way to achieve NIR absorption.^[13] Although these methods can greatly enhance the Q-band absorption compared with that of the porphyrin monomer, it is usually difficult to achieve very intense absorption beyond 1000 nm with a molar extinction coefficient (ϵ) larger than $1.0 \times 10^5 \text{ M}^{-1} \text{ cm}^{-1}$. On the other hand, rylene, the *peri*-condensed naphthalene oligomer, forms the basis of a family of important organic dyes, showing intense red-shifted p-band absorption with extension of the molecular length as the S_0 – S_1 electronic transition moment lies along the long molecular axis (x-axis in Figure 1).^[14] For example, a hexarylenebis(dicarboximide) dye exhibits an intense absorption ($\epsilon = 2.93 \times 10^5 \text{ M}^{-1} \text{ cm}^{-1}$) with a maximum at 953 nm.^[14f] However, the synthesis of even longer rylene molecules with absorption beyond 1000 nm is very challenging.^[14g] Detailed photophysical studies on triply fused porphyrin tapes have revealed that the position of the longest-wavelength absorption band (Q-band) is correlated with the S_0 – S_1 electronic transition along the long molecular axis (x-axis in Figure 1).^[15] Therefore, we envisaged that fusion

[a] Dr. J. Luo, Dr. G. Li, Prof. J. Wu

Institute of Materials Research and Engineering (IMRE)
A*STAR (Agency for Science, Technology and Research)
3 Research Link, Singapore 117602 (Singapore)
Fax: (+65) 67791691
E-mail: chmwuj@nus.edu.sg

[b] S. Lee, M. Son, Prof. D. Kim

Department of Chemistry, Yonsei University
Seoul 120-749 (Korea)
E-mail: dongho@yonsei.ac.kr

[c] Dr. B. Zheng, Prof. K.-W. Huang

Division of Physical Sciences and Engineering, KAUST Catalysis Center
King Abdullah University of Science and Technology (KAUST)
Thuwal 23955-6900 (Saudi Arabia)

[d] Q. Qi, W. Zeng, Prof. J. Wu

Department of Chemistry, National University of Singapore
3 Science Drive 3, Singapore 117543 (Singapore)

Supporting information for this article is available on the WWW under
<http://dx.doi.org/10.1002/chem.201405574>.

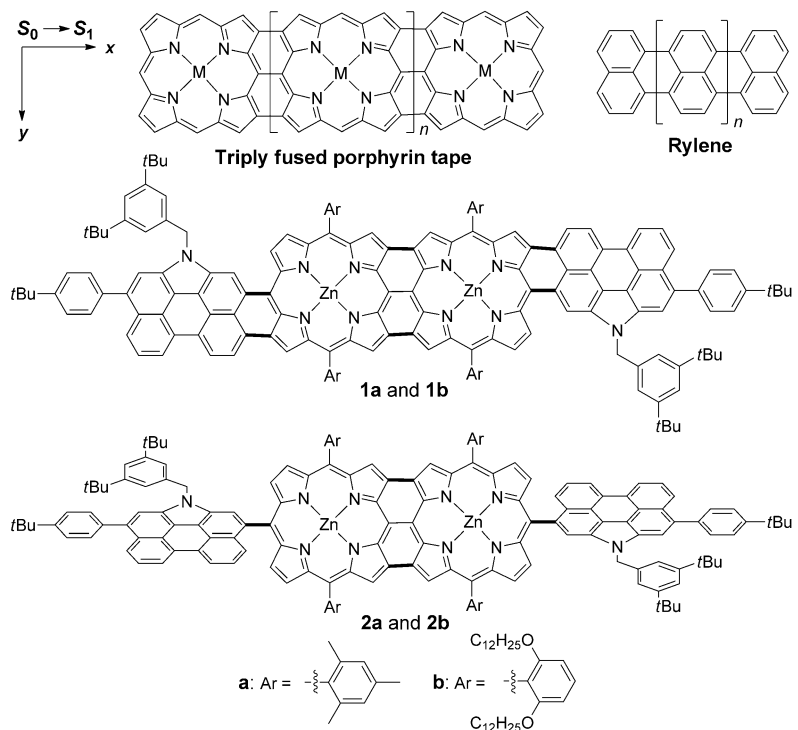
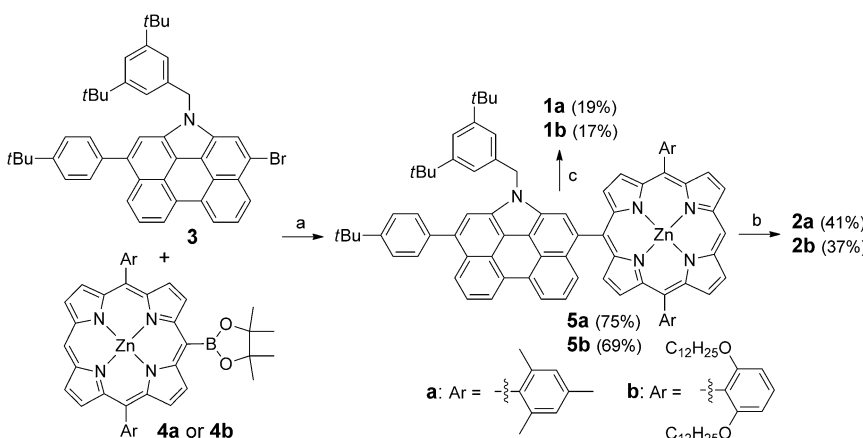


Figure 1. Structures of *meso*, β , β' -triply fused porphyrin tape, rylene, and the perylene-fused and substituted porphyrin dimers **1a/1b** and **2a/2b**.

of a rylene moiety with a triply fused porphyrin along the same S_0-S_1 electronic transition moment axis (x -axis) could result in greatly enhanced Q-band absorption in the NIR region well beyond 1000 nm. Our preliminary studies showed that perylene-fused porphyrin monomers indeed displayed intense NIR absorption ($\epsilon > 1.0 \times 10^5 \text{ M}^{-1} \text{ cm}^{-1}$), but the absorption maximum was still at less than 1000 nm.^[16] To further validate our assumption, in this work, *N*-annulated perylene (NP)-fused porphyrin dimers **1a/1b** have been synthesized and their photophysical properties have been investigated in detail (Figure 1). NP was chosen mainly because of its electron-rich character,^[17] which is comparable to that of Zn-porphyrin and allows us to generate fused systems by oxidative cyclodehydrogenation. Different aryl substituents (mesityl and 2,6-didodecyloxyphenyl) were introduced on the central fused porphyrin dimer to control possible molecular aggregation as well as solubility. The partially fused NP-substituted porphyrin dimers **2a/2b** were also obtained by controlling the reaction conditions and serve as good references for the fully fused NP-porphyrin tapes **1a/1b**. Our detailed studies support our design concept, and new NIR dyes with very intense ab-



Scheme 1. Synthesis of *N*-annulated perylene-substituted and fused porphyrin dimers **1a/1b** and **2a/2b**: (a) $\text{Pd}(\text{PPh}_3)_4$, aq. K_2CO_3 , toluene, 95°C ; (b) 5 equiv $\text{Sc}(\text{OTf})_3$, DDQ, toluene, 50°C ; (c) 5 equiv $\text{Sc}(\text{OTf})_3$, DDQ, toluene, 90°C .

dicyano-1,4-benzoquinone),^[18] and the latter method successfully promoted the reaction in reasonable yield. By carefully controlling the reaction temperature and amount of oxidant, both the partially fused **2a/2b** and the fully fused NP-porphyrin tapes **1a/1b** could be obtained in reasonable yields. A higher reaction temperature (90°C) led to the fully fused NP-porphyrin tapes **1a/1b**, whereas a lower temperature (50°C) mainly gave the NP-substituted fused porphyrin dimers **2a/2b**. All products were well characterized by 1D and 2D NMR techniques and high-resolution mass spectrometry (see the Supporting Information). The 2,6-didodecyloxyphenyl-substituted

sorption beyond 1250 nm have been obtained, which also show large TPA cross-sections.

Results and Discussion

Synthesis

The synthetic route towards *N*-annulated perylene-substituted and fused porphyrin dimers is shown in Scheme 1. The NP-substituted porphyrin monomers **5a/5b** were prepared by Suzuki coupling between the monobromo-substituted *N*-annulated perylene **3**^[16a] and the porphyrin monoboronic ester **4**.^[16c] The key step in the synthesis was the subsequent formation of the triply linked porphyrin dimer. Oxidative couplings and cyclodehydrogenations of **5a/5b** were attempted using PIFA ([bis(trifluoroacetoxy)iodo]benzene)^[17] and $\text{Sc}(\text{OTf})_3/\text{DDQ}$ (2,3-dichloro-5,6-

porphyrin dimers **1b/2b** showed better resolved NMR spectra and higher solubility than the corresponding mesityl-substituted compounds **1a/2a** due to efficient suppression of molecular aggregation in solution. It should be noted that only one isomer was observed for the fully fused diporphyrins based on NMR analysis, which is consistent with the previous report by Osuka et al.^[13e] According to previous studies on the synthesis of arene-fused porphyrins by oxidative coupling, we propose that the *anti*-regioisomer is the most likely product formed in our reaction,^[13,19] but crystallographic analysis of these compounds proved to be very challenging.

Steady-state absorption and emission spectra

Steady-state absorption spectra of the NP-fused diporphyrins **1a/1b** and the NP-substituted diporphyrins **2a/2b** in dichloromethane are shown in Figure 2 and the data are collected in Table 1. The NP-substituted porphyrin dimers **2a** and **2b** show intense absorption bands at 413 and 416 nm, as well as shoulders around 454 and 455 nm, respectively. Such an absorption feature can be attributed to the superimposition of the Soret band I of the fused Zn-porphyrin dimer^[15] and the p-band of the NP chromophore.^[17] Moreover, **2a** and **2b** exhibit strongly red-shifted Soret band II around 591 and 593 nm, respectively, as well as relatively weak Q-bands at 1061 and 1045 nm, respectively. Both the Soret band II and the Q-band are similar to those observed for the fused Zn-porphyrin dimer.^[15] A slight hypsochromic shift in the absorption spectrum of **2b** bearing 2,6-didodecyloxyphenyl substituents was observed in comparison with that of **2a** bearing mesityl substituents. In contrast, the

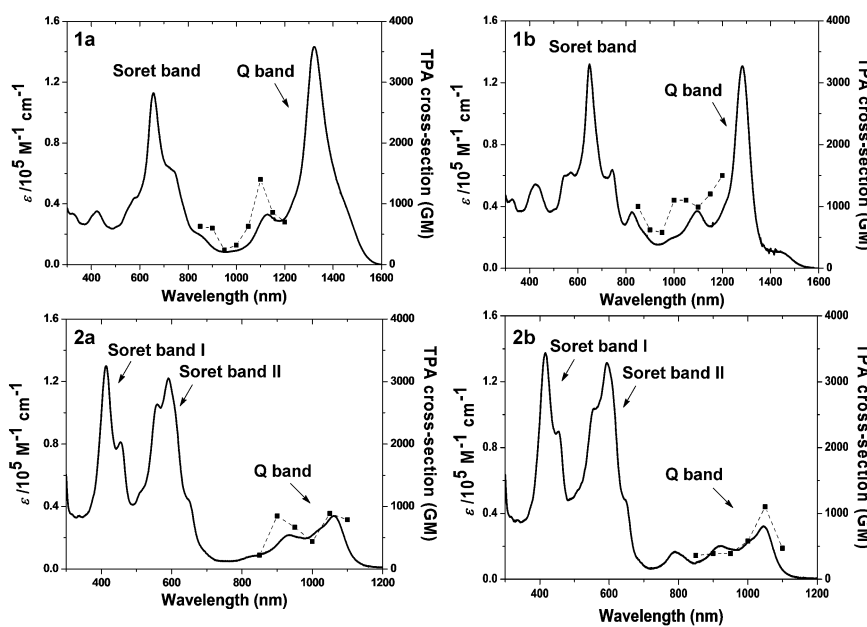


Figure 2. OPA (solid line and left vertical axis) and TPA spectra (dashed line and right vertical axis) of **1a/1b** and **2a/2b** in CH_2Cl_2 . The TPA spectra are plotted at $\lambda_{\text{ex}}/2$ for comparison between the OPA and TPA spectra.

Table 1. Summary of optical and electrochemical properties of NP-functionalized porphyrin dimers **1a/1b** and **2a/2b**.

Dye	λ_{abs} [nm]	ϵ $[\text{M}^{-1} \text{cm}^{-1}]$	E_g^{opt} [eV]	$E_{1/2}^{\text{ox}}$ [V]	$E_{1/2}^{\text{red}}$ [V]	HOMO [eV]	LUMO [eV]	E_g^{EC} [eV]	τ [ps]	$\sigma^{(2)}_{\text{max}}$ [GM]
1a	421	35200	0.78	0.17	-0.57	-4.35	-3.73	0.62	6.0	1400 (2200 nm)
	657	112800		0.37	-0.81					
	746	60400		0.96						
	1128	32900		1.06						
	1322	143200		1.27						
	1447	41100		1.51						
	424	54250	0.81	0.15	-0.69	-4.36	-3.61	0.75	8.1	1500 (2400 nm)
1b	649	132000		0.41	-0.89					
	744	63750		0.90						
	824	36500		1.01						
	1096	37000		1.13						
	1283	130750		1.38						
	1450	10250								
	413	130000	1.06	0.56	-0.55	-4.79	-3.75	1.04	4.4	890 (2100 nm)
2a	454	81200		0.77	-0.81					
	559	105400		0.97						
	591	122000		1.34						
	934	21800								
	1061	34000								
	416	137400	1.09	0.47	-0.78	-4.69	-3.56	1.13	4.9	1100 (2100 nm)
	455	89700		0.80	-0.97					
2b	555	103500		1.00						
	593	131500		1.36						
	920	20200								
	1045	32200								

λ_{abs} : absorption maximum measured in CH_2Cl_2 . ϵ : molar extinction coefficient in units of $\text{M}^{-1} \text{cm}^{-1}$. E_g^{opt} : optical energy gap derived from lowest energy absorption onset in the absorption spectra. $E_{1/2}^{\text{ox}}$ and $E_{1/2}^{\text{red}}$ are the half-wave potentials of the oxidative and reductive waves, respectively, with potentials vs AgCl/Ag reference. HOMO and LUMO energy levels were calculated according to the equations: $\text{HOMO} = -(4.8 + E_{\text{ox}}^{\text{onset}} - E_{1/2}(\text{Fc}^+/\text{Fc}))$ and $\text{LUMO} = -(4.8 + E_{\text{red}}^{\text{onset}} - E_{1/2}(\text{Fc}^+/\text{Fc}))$, where $E_{\text{ox}}^{\text{onset}}$ and $E_{\text{red}}^{\text{onset}}$ are the onset potentials of the first oxidative and reductive redox waves, respectively, and $E_{1/2}(\text{Fc}^+/\text{Fc})$ is the half-wave potential of ferrocene with respect to the same reference (0.54 V in this case). E_g^{EC} : electrochemical energy gap derived from LUMO–HOMO. τ is the singlet excited-state lifetime obtained from TA. $\sigma^{(2)}_{\text{max}}$ is the maximum TPA cross-section.

Soret bands of NP-fused diporphyrins **1a** and **1b** appeared as one broad absorption and were red-shifted to 657 and 649 nm, respectively, due to extension of the conjugation to the entire molecules. The differences in the Q-bands between **1a/1b** and **2a/2b** were even more distinct. Upon fusion of two additional NP units at the periphery of the porphyrin dimer, the Q-bands of **1a** and **1b** were significantly red-shifted to 1322 and 1283 nm, respectively. Remarkably, their absorption intensities were considerably increased, with molar extinction coefficients larger than $1.3 \times 10^5 \text{ M}^{-1} \text{ cm}^{-1}$ (Table 1). The highly rigid molecular structures imposed by complete fusion of the chromophores cause the transition dipole moments of the NP and porphyrin moieties to lie parallel to the direction of the long molecular axis, making the Q-bands much more intense than those of the partially fused analogues. The optical energy gaps (E_g^{opt}) of **1a**, **1b**, **2a**, and **2b** were estimated from the absorption onsets as 0.78, 0.81, 1.06, and 1.09 eV, respectively.

The steady-state fluorescence spectra of **1a/1b** and **2a/2b** were also measured and showed distinctive features. Whereas no fluorescence was observed from diporphyrins **2a** and **2b**, **1a** and **1b** exhibited moderate NIR fluorescence with maxima at 1342 and 1315 nm, respectively (Figure 3). Small Stokes

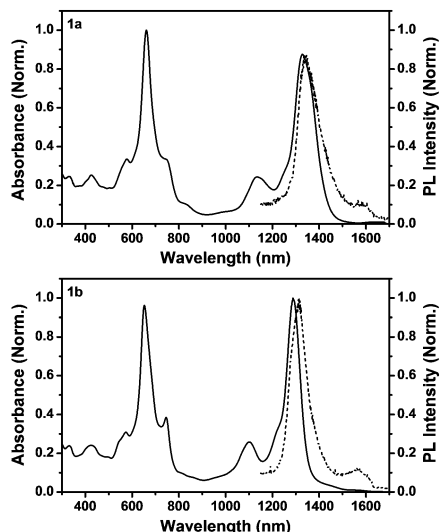


Figure 3. Normalized UV/Vis/NIR absorption (solid lines) and emission spectra (dashed lines) of **1a/1b** in CH_2Cl_2 .

shifts (20 nm for **1a**; 32 nm for **1b**) were determined, indicating minimal structural changes in the singlet excited states of these rigid π -conjugated systems. The fluorescence quantum yields were determined as 4.4×10^{-6} for **1a** and 6.0×10^{-6} for **1b** by using [26]hexaphyrin (quantum yield $\approx 10^{-4}$) as a reference molecule.^[11a,15] Although the phenyl-terminated fused Zn-porphyrin dimer showed fluorescence with a quantum yield of around 2×10^{-5} ,^[15] the NP-terminated porphyrin dimers **2a/2b** were seen to be almost non-luminescent, presumably due to enhanced non-radiative decay of the first excited state upon geometric change or intramolecular charge transfer.

We also measured the thin-film absorption spectra of compounds **1a/1b** and **2a/2b** (Figure S2 in the Supporting Information), which were generally similar to the solution-based UV/Vis/NIR spectra. However, due to strong aggregation in the solid state, these spectra were considerably red-shifted and featured long tails.

Transient absorption and two-photon absorption spectra

The excited-state dynamics of **1a/1b** and **2a/2b** was investigated by femtosecond transient absorption (TA) spectroscopic measurements in toluene. Interestingly, all of the compounds showed similar TA spectral features to those of the previously reported fused Zn-porphyrin dimer, except for differences in wavelengths (Figure 4).^[15] **1a** showed an intense ground-state bleaching (GSB) signal at 662 nm, originating from the Soret band, and two excited-state absorption (ESA) bands in the 750–1120 and 1150–1300 nm spectral regions, whereas **2a** exhibited two GSB signals at 560 and 1075 nm (correlated with the Soret and Q-bands, respectively) and two ESA bands at 630–1000 and 1130–1300 nm. Similar TA spectra were obtained for **1b** and **2b**. The singlet excited-state lifetimes (τ) were measured as 6.0 and 8.1 ps for **1a** and **1b**, respectively, whereas **2a** and **2b** displayed slightly shorter lifetimes of 4.4 and 4.9 ps (Figure 4). The larger τ values for the fully fused porphyrin dimers (**1a/1b**) compared with those of the corresponding partially fused porphyrin dimers (**2a/2b**) could be explained in terms of their more rigid structures, which is also consistent with the steady-state fluorescence results. In other words, activation of the non-radiative decay channel due to the structural flexibility of **2a** and **2b** leads to decreases in the singlet excited-state lifetimes as compared to those of their fused counterparts.

TPA measurements were conducted for **1a/1b** and **2a/2b** by using the open-aperture Z-scan method with excitation wavelengths (λ_{ex}) in the region 1700–2400 nm, in which the contribution from one-photon absorption is negligible (Figure 2). The maximum TPA cross-sections ($\sigma^{(2)}$) of **2a/2b** were measured as 890 and 1100 GM at 2100 nm, respectively. Due to the limited excitation wavelength range (ca. 2400 nm) of our set-up, we could only obtain the TPA spectra of **1a/1b** at the shoulder regions of their Q-bands, which still showed large $\sigma^{(2)}$ values with maxima of 1400 GM at 2200 nm for **1a** and 1500 GM at 2400 nm for **1b**. Based on the observed trends, much larger $\sigma^{(2)}$ values can be predicted for **1a/1b** in the longer-wavelength region of the Q-bands. Such high non-linear susceptibilities, reflected in the large measured TPA cross-sections, can be ascribed to the highly delocalized nature of their π -conjugated frameworks. Larger TPA cross-sections measured for **1a** and **1b** reflect the fact that these NP-fused dimers are more extensively π -conjugated than **2a** and **2b**, as also suggested by their highly red-shifted Q-bands.

Electrochemical properties

The electrochemical properties of **1a/1b** and **2a/2b** were investigated by cyclic voltammetry (CV) and differential pulse

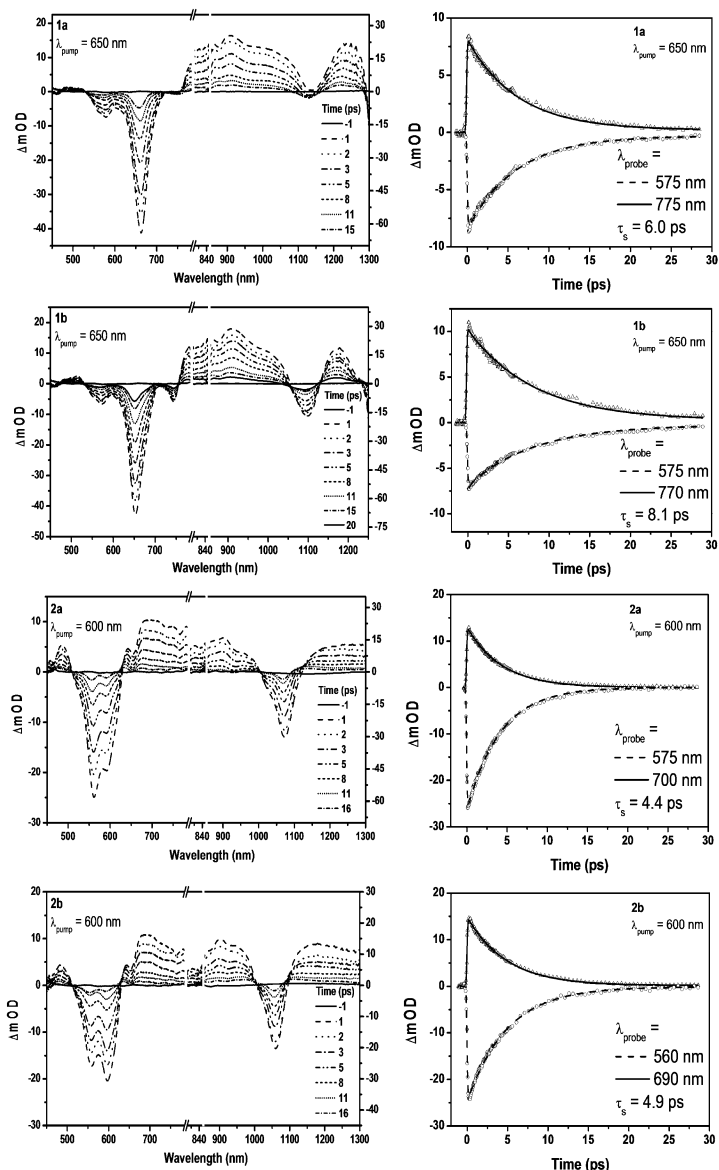


Figure 4. Transient absorption spectra (left) and decay curves (right) of compounds **1a/1b** and **2a/2b** in toluene.

voltammetry (DPV) in deoxygenated CH_2Cl_2 solution containing 0.1 M tetra-*n*-butylammonium hexafluorophosphate (TBAPF₆) as supporting electrolyte (Figure 5 and Figure S2). Multiple redox waves were observed for all four compounds (see the list of half-wave potentials $E_{1/2}^{\text{ox}}$ (anodic scan) and $E_{1/2}^{\text{red}}$ (cathodic scan) in Table 1). The HOMO and LUMO energy levels were estimated from the onsets of the first oxidation and reduction waves,^[20] and amounted to -4.35 , -4.36 , -4.79 , and -4.69 eV (HOMO) and -3.73 , -3.61 , -3.75 , and -3.56 eV (LUMO) for **1a**, **1b**, **2a**, and **2b**, respectively. Accordingly, the electrochemical energy gaps (E_g^{EC}) were calculated as 0.62, 0.75, 1.04, and 1.13 eV, respectively, which are consistent with the optical energy gaps. Thus, it can be concluded that fusion of an NP unit onto the porphyrin core (in **1a/1b**) significantly elevates the HOMO energy levels compared to those of the NP-substituted porphyrins **2a/2b**, leading to narrower energy gaps.

DFT calculations

Density functional theory (DFT, B3LYP/6-31G*) calculations were conducted to better understand the electronic and optical properties of **1a/1b** and **2a/2b**. The calculated frontier HOMO and LUMO profiles and energy levels are shown in Figure 6. Upon fusion, both the HOMO and LUMO energy levels were increased, resulting in a smaller energy gap, which is consistent with the experimental data. Interestingly, whereas the HOMO and LUMO coefficients of **2a** and **2b** are mainly localized on the central diporphyrin moiety, the frontier molecular orbitals of the fully fused dimers **1a** and **1b** revealed delocalization of electron density to the peripheral NP moieties, which is consistent with our experimental findings. The 2,6-didodecyloxyphenyl-substituted compounds **1b/2b** show higher-lying HOMO/LUMO energy levels compared with those of the corresponding mesityl-substituted compounds **1a/2a** due to the electron-donating property of the alkoxy chains. Time-dependent DFT calculations predicted HOMO \rightarrow LUMO electronic transition bands at 1293.2 nm (oscillator strength $f=1.6463$), 1162.9 nm ($f=1.7353$), 1029.1 nm ($f=0.4261$), and 919.1 nm ($f=0.4660$) for **1a**, **1b**, **2a**, and **2b**, respectively (see the Supporting Information), and the trend is consistent with the experimental data.

Conclusion

N-annulated perylene-substituted and fused Zn-porphyrin dimers have been successfully synthesized by a regioselective oxidative coupling/cyclodehydrogenation strategy. Since the fusion is along the S_0 - S_1 transition moment axis of both the fused porphyrin dimer and the perylene, the obtained fused dyes **1a/1b** and **2a/2b** show very intense absorption beyond 1250 nm.

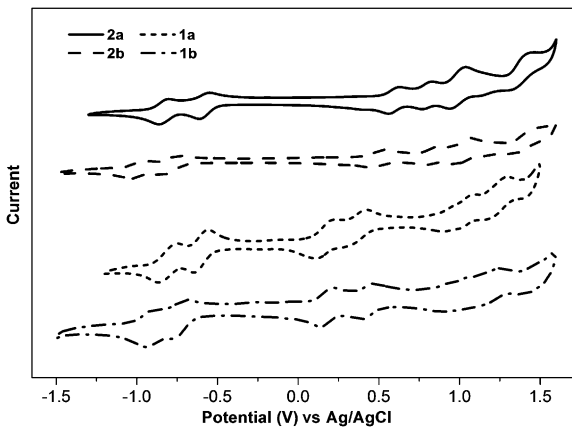


Figure 5. Cyclic voltammograms of **1a/1b** and **2a/2b** in dry CH_2Cl_2 with TBAPF₆ as supporting electrolyte, AgCl/Ag as reference electrode, an Au disk as working electrode, a Pt wire as counter electrode, and a scan rate of 50 mV s⁻¹.

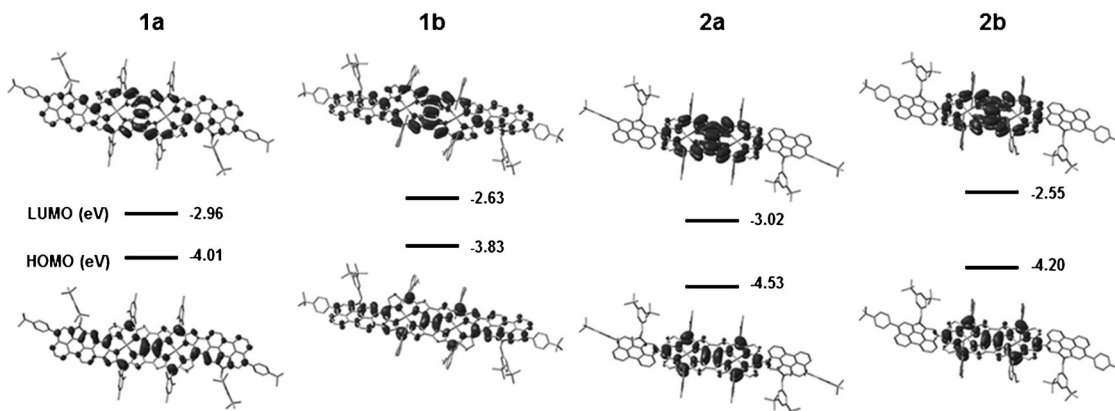


Figure 6. Calculated frontier molecular orbital profiles and energy levels for **1a/1b** and **2a/2b**. The long alkoxy chains in **1b** and **2b** were replaced by ethoxy groups to reduce the calculation cost and time.

Due to the extended π -conjugation, large TPA cross-sections were obtained, and thus these materials represent new high-performance NIR dyes and TPA chromophores for applications such as NIR photodetection and light saturation at telecommunication wavelengths. Our research provides guidance for obtaining NIR dyes with very intense absorption at longer wavelengths in the NIR region. Experiments aimed at further extending the π -conjugated system based on this concept are currently underway.

Experimental Section

Synthesis of compounds **5a/5b**

Perylene **3** (271.5 mg, 0.4 mmol), porphyrin **4a/4b** (0.4 mmol), Pd(PPh₃)₄ (46 mg, 0.04 mmol), and Cs₂CO₃ (260 mg, 0.8 mmol) were dried under vacuum and then purged with argon. Degassed toluene (10 mL) and DMF (5 mL) were then added, and the mixture was stirred at 96 °C for 36 h. After cooling, water was added and the product was extracted with CH₂Cl₂ (3 × 30 mL). The organic layer was washed with saturated brine and dried over anhydrous Na₂SO₄. The solvent was removed under vacuum, and the residue was purified by column chromatography (silica gel; CH₂Cl₂/hexane, 1:3) to give the coupling product **5a/5b** as a purple solid.

5a:^[16c] Yield: 75%; ¹H NMR (CDCl₃, 400 MHz): δ = 10.21 (s, 1 H), 9.37 (d, J = 4.5 Hz, 2 H), 8.93 (d, J = 4.4 Hz, 2 H), 8.77 (m, 3 H), 8.69 (m, 3 H), 8.54 (s, 1 H), 8.30 (d, J = 8.4 Hz, 1 H), 7.88 (dd, J = 15.1, 6.9 Hz, 2 H), 7.73 (d, J = 8.1 Hz, 2 H), 7.63 (d, J = 8.2 Hz, 2 H), 7.46 (m, 1 H), 7.30–7.21 (m, 8 H), 5.98 (s, 2 H), 2.63 (s, 6 H), 1.89 (s, 6 H), 1.83 (s, 6 H), 1.49 (s, 9 H), 1.12 ppm (s, 18 H); ¹³C NMR (100 MHz, CDCl₃): δ = 151.37, 151.10, 150.07, 149.99, 149.91, 149.69, 139.29, 139.08, 138.92, 138.02, 137.43, 137.06, 136.59, 133.56, 132.61, 132.53, 132.37, 132.06, 131.31, 131.21, 130.83, 130.39, 129.99, 128.20, 127.68, 127.61, 126.57, 125.35, 125.15, 124.77, 124.41, 123.47, 121.94, 121.68, 121.23, 120.50, 120.28, 118.92, 118.74, 117.98, 117.34, 114.71, 105.41, 50.41, 34.70, 31.53, 31.32, 21.75, 21.62, 21.45 ppm; HRMS (APCI): m/z = 1206.5387 (M^+ +1); elemental analysis calcd (%) for C₈₃H₇₆N₅Zn: 1206.5399 (error = -1.0 ppm).

5b: Yield: 69%; ¹H NMR (500 MHz): δ = 10.14 (s, 1 H), 9.31 (d, J = 4.5 Hz, 2 H), 9.03 (d, J = 4.4 Hz, 2 H), 8.78 (d, J = 4.6 Hz, 2 H), 8.76 (s, 1 H), 8.75 (d, J = 4.6 Hz, 2 H), 8.66 (s, 1 H), 8.65 (d, J = 7.6 Hz, 1 H), 8.28 (d, J = 8.5 Hz, 1 H), 7.85 (dd, J = 8.5, 7.4 Hz, 1 H), 7.83 (s, 1 H),

7.71 (d, J = 8.4 Hz, 2 H), 7.67 (t, J = 8.5 Hz, 2 H), 7.61 (d, J = 8.4 Hz, 2 H), 7.38 (dd, J = 8.4, 7.4 Hz, 1 H), 7.27 (m, 3 H), 7.15 (d, J = 8.4 Hz, 1 H), 6.99 (dd, J = 8.5, 1.7 Hz, 4 H), 5.98 (s, 2 H), 3.83 (td, J = 6.6, 3.7 Hz, 8 H), 1.49 (s, 9 H), 1.17 (s, 18 H), 1.12–0.35 ppm (m, 92 H); ¹³C NMR (126 MHz): δ = 160.11, 160.07, 151.34, 150.66, 150.57, 149.96, 149.39, 139.19, 137.94, 137.69, 136.75, 133.80, 132.43, 131.71, 131.63, 131.45, 131.21, 131.13, 130.30, 129.99, 129.57, 128.18, 125.29, 125.17, 124.67, 124.56, 121.73, 121.57, 121.53, 119.68, 118.00, 117.78, 117.50, 112.82, 105.33, 105.27, 68.69, 68.53, 34.74, 34.68, 31.83, 31.82, 31.53, 31.44, 31.36, 30.21, 29.69, 29.44, 29.43, 29.33, 29.22, 29.21, 29.17, 29.02, 29.00, 28.66, 28.62, 28.58, 28.47, 25.13, 25.07, 22.60, 14.06, 14.05 ppm; HRMS (APCI): m/z = 1859.1759 (M^+ +1); elemental analysis calcd (%) for C₁₂₅H₁₆₀N₅O₄Zn: 1859.1756 (error = +0.2 ppm).

General procedure for the synthesis of diporphyrins **1a/1b/2a/2b**

Argon was bubbled through a solution of porphyrin-NP dyad **5a/b** (50 mg) in dry toluene (25 mL) for 10 min and then DDQ (5 equiv) and Sc(OTf)₃ (5 equiv) were added. The reaction mixture was heated and stirred under Ar for some additional time (50 °C for 2 h for diporphyrins **2a/2b**; 90 °C for 5 h for diporphyrins **1a/b**). THF (5 mL) was then added to quench the reaction and the mixture was stirred for a further 1 h. The mixture was then passed through a short neutral alumina column and the solvent was removed. The residue was further purified on a second neutral alumina column (THF/CH₂Cl₂, 1:1, as eluent). After washing with MeOH, the porphyrin dimers **2a/2b** and **1a/b** were obtained as dark-purple solids.

1a: Yield: 19%; ¹H NMR (400 MHz, CDCl₃): δ = 9.18–8.91 (m, 4 H), 8.86 (br, 2 H), 8.73 (br, 2 H), 8.53 (br, 2 H), 8.25 (d, 2 H), 8.05 (br, 2 H), 7.88 (m, 2 H), 7.75 (br, 4 H), 7.64 (s, 4 H), 7.59 (s, 4 H), 7.37 (br, 4 H), 7.23–7.12 (m, 5 H), 6.97 (s, 2 H), 6.93 (s, 2 H), 5.99 (s, 4 H), 2.59 (d, J = 17.2 Hz, 12 H), 2.13 (s, 24 H), 1.45 (s, 18 H), 1.17 ppm (s, 36 H); HRMS (MALDI-TOF): m/z = 2400.9882 (M^+); elemental analysis calcd (%) for C₁₆₆H₁₄₀N₁₀Zn₂: 2400.9840 (error = +1.75 ppm).

1b: Yield: 17%; ¹H NMR (400 MHz, C₆D₆): δ = 8.73 (d, J = 7.9 Hz, 2 H), 8.72 (s, 2 H), 8.64 (d, J = 7.2 Hz, 2 H), 8.56 (d, J = 5.5 Hz, 2 H), 8.42 (d, J = 7.9 Hz, 2 H), 8.37 (d, J = 8.1 Hz, 2 H), 8.10 (m, 2 H), 7.94 (d, J = 4.3 Hz, 2 H), 7.77 (d, J = 7.1 Hz, 4 H), 7.70 (m, 2 H), 7.59 (s, 2 H), 7.58 (s, 2 H), 7.54 (d, J = 8.1 Hz, 4 H), 7.52–7.42 (m, 12 H), 6.78 (dd, J = 13.5, 8.6 Hz, 8 H), 5.57 (s, 4 H), 3.86 (m, 16 H), 1.38 (s, 18 H), 1.30 (s, 36 H), 1.25–0.65 ppm (m, 184 H); HRMS (MALDI-TOF): m/z =

3707.4606 ($M^+ + 1$); elemental analysis calcd (%) for $C_{250}H_{309}N_{10}O_8Zn_2$: 3707.2657.

2a: Yield: 41%; 1H NMR (400 MHz, $CDCl_3$): $\delta = 8.75$ (d, $J = 7.6$ Hz, 2H), 8.67 (d, $J = 7.3$ Hz, 2H), 8.24 (d, $J = 8.4$ Hz, 2H), 8.15 (s, 2H), 7.84 (d, $J = 6.0$ Hz, 4H), 7.67 (t, $J = 6.1$ Hz, 6H), 7.61 (t, $J = 6.9$ Hz, 6H), 7.45 (d, $J = 4.5$ Hz, 4H), 7.33 (d, $J = 4.5$ Hz, 4H), 7.23 (s, 4H), 7.09 (s, 8H), 6.94 (s, 4H), 5.92 (s, 4H), 2.49 (s, 12H), 2.06 (s, 12H), 2.03 (s, 12H), 1.47 (s, 18H), 1.15 ppm (s, 36H); ^{13}C NMR (100 MHz, $CDCl_3$): $\delta = 154.27$, 154.13, 153.46, 152.99, 151.41, 150.08, 139.03, 138.43, 138.06, 137.09, 136.39, 135.30, 132.52, 131.38, 130.68, 129.95, 129.88, 128.15, 127.63, 127.56, 125.31, 125.03, 124.87, 124.70, 123.89, 123.16, 121.80, 121.67, 121.17, 120.68, 119.13, 117.87, 117.17, 116.96, 114.58, 50.37, 31.51, 31.35, 30.23, 29.69, 21.37, 21.26 ppm; HRMS (APCI): $m/z = 2406.0249$ ($M^+ + 1$); elemental analysis calcd (%) for $C_{166}H_{145}N_{10}Zn_2$: 2406.0231 (error = +0.7 ppm).

2b: Yield: 37%; 1H NMR (400 MHz, $CDCl_3$): $\delta = 8.74$ (d, $J = 7.6$ Hz, 2H), 8.65 (d, $J = 7.4$ Hz, 2H), 8.27 (s, 2H), 8.24 (d, $J = 8.4$ Hz, 4H), 7.82 (t, $J = 7.8$ Hz, 2H), 7.76 (s, 2H), 7.67 (m, 4H), 7.64–7.54 (m, 10H), 7.51–7.42 (m, 12H), 7.29 (s, 2H), 7.23 (s, 4H), 7.11 (s, 4H), 6.79 (d, $J = 7.8$ Hz, 8H), 5.92 (s, 4H), 3.89 (m, 16H), 1.47 (s, 18H), 1.19 (s, 36H), 1.25–0.71 ppm (m, 184H); ^{13}C NMR (100 MHz, $CDCl_3$): $\delta = 159.36$, 154.14, 154.01, 153.47, 151.30, 149.91, 139.12, 137.57, 136.70, 136.40, 136.21, 132.28, 132.06, 131.50, 130.84, 130.74, 130.31, 129.94, 129.16, 128.06, 126.13, 125.26, 125.01, 124.61, 124.45, 123.97, 123.84, 121.73, 121.51, 120.90, 120.52, 119.86, 119.10, 117.71, 117.54, 117.30, 117.04, 114.72, 104.96, 68.84, 68.64, 50.21, 34.73, 31.92, 31.81, 31.51, 31.35, 30.18, 29.69, 29.61, 29.50, 29.28, 29.11, 28.98, 28.79, 25.75, 25.57, 22.69, 22.52, 14.04 ppm; HRMS (ESI): $m/z = 1855.1430$ ($M^+ + 2$); elemental analysis calcd (%) for $C_{250}H_{312}N_{10}O_8Zn_2$: 1855.1443 (error: -0.7 ppm).

More experimental/theoretical calculation details and data are available in the Supporting Information.

Acknowledgements

J.W. acknowledges financial support from MOE Tier 2 grants (MOE2011-T2-2-130, MOE2014-T2-1-080) and an A*STAR JCO grant (1431AFG100). The work at Yonsei University was financially supported by the Mid-career Researcher Program (2005-0093839) and Global Research Laboratory (2013K1A1A2A02050183) administered through the National Research Foundation of Korea (NRF) funded by the Ministry of Education, Science and Technology (MEST). K.-W.H. is grateful for financial support from KAUST.

Keywords: near-infrared dye • nonlinear optics • porphyrinoids • rylene • transient absorption • two-photon absorption

- [1] a) P. Peumans, A. Yakimov, S. R. Forrest, *J. Appl. Phys.* **2003**, *93*, 3693–3723; b) H. Imahori, T. Umeyama, S. Ito, *Acc. Chem. Res.* **2009**, *42*, 1809–1818; c) M. D. Perez, C. Borek, P. I. Djurovich, E. I. Mayo, R. R. Lunt, S. R. Forrest, M. E. Thompson, *Adv. Mater.* **2009**, *21*, 1517–1520; d) M. G. Walter, A. B. Rudine, C. C. Wamser, *J. Porphyrins Phthalocyanines* **2010**, *14*, 759–792; e) L.-L. Li, E. W.-G. Diau, *Chem. Soc. Rev.* **2013**, *42*, 291–304.
- [2] A. Tsuda, A. Osuka, *Adv. Mater.* **2002**, *14*, 75–79.
- [3] M. O. Senge, M. Fazekas, E. G. A. Notaras, W. J. Blau, M. Zawadzka, O. B. Locos, E. M. N. Mhuircheartaigh, *Adv. Mater.* **2007**, *19*, 2737–2774.

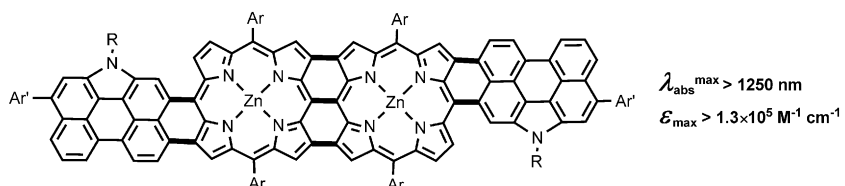
- [4] a) M. Biesaga, K. Pyrzyńska, M. Trojanowicz, *Talanta* **2000**, *51*, 209–224; b) D. Monti, S. Nardis, M. Stefanelli, R. Paolesse, C. D. Natale, A. D'Amico, *J. Sens.* **2009**, DOI: 10.1155/2009/856053; c) S. Ishihara, J. Labuta, W. V. Rossom, D. Ishikawa, K. Minami, J. P. Hill, K. Ariga, *Phys. Chem. Chem. Phys.* **2014**, *16*, 9713–9746; d) Y.-Y. Lv, S.-W. Wu, J. Li, *Curr. Org. Chem.* **2014**, *18*, 475–488.
- [5] a) K. S. Kim, J. M. Lim, A. Osuka, D. Kim, *J. Photochem. Photobiol. C* **2008**, *9*, 13–28; b) M. Pawlicki, H. A. Collins, R. G. Denning, H. L. Anderson, *Angew. Chem. Int. Ed.* **2009**, *48*, 3244–3266; *Angew. Chem.* **2009**, *121*, 3292–3316; c) L. T. Bergendahl, M. J. Paterson, *RSC Adv.* **2013**, *3*, 9247–9257.
- [6] a) H. T. Uyeda, Y. Zhao, K. Wostyn, I. Asselberghs, K. Clays, A. Persoons, M. J. Therien, *J. Am. Chem. Soc.* **2002**, *124*, 13806–13813; b) M. Drobizhev, Y. Stepanenko, Y. Dzenis, A. Karotki, A. Rebane, P. N. Taylor, H. L. Anderson, *J. Am. Chem. Soc.* **2004**, *126*, 15352–15353; c) M. Drobizhev, Y. Stepanenko, Y. Dzenis, A. Karotki, A. Rebane, P. N. Taylor, H. L. Anderson, *J. Phys. Chem. B* **2005**, *109*, 7223–7236; d) J. T. Dy, R. Maeda, Y. Nagatsuka, K. Ogawa, K. Kamada, K. Ohta, Y. Kobuke, *Chem. Commun.* **2007**, 5170–5172; e) J. A. N. Fisher, K. Susumu, M. J. Therien, A. G. Yodh, *J. Chem. Phys.* **2009**, *130*, 134506–134514; f) E. Dahlstedt, H. A. Collins, M. Balaz, M. K. Kuimova, M. Khurana, B. C. Wilson, D. Phillips, H. L. Anderson, *Org. Biomol. Chem.* **2009**, *7*, 897–904; g) S. Achelle, P. Couleaud, P. Baldeck, M.-P. Teulade-Fichou, P. Maillard, *Eur. J. Org. Chem.* **2011**, 1271–1279.
- [7] a) M. J. Frampton, H. Akdas, A. R. Cowley, J. E. Rogers, J. E. Slagle, P. A. Fleitz, M. Drobizhev, A. Rebane, H. L. Anderson, *Org. Lett.* **2005**, *7*, 5365–5368; b) M. Drobizhev, F. Meng, A. Rebane, Y. Stepanenko, E. Nickel, C. W. Spangler, *J. Phys. Chem. B* **2006**, *110*, 9802–9814.
- [8] See review: J. P. Lewtak, D. T. Gryko, *Chem. Commun.* **2012**, *48*, 10069–10086.
- [9] C. Ikeda, Z. S. Yoon, M. Park, H. Inoue, D. Kim, A. Osuka, *J. Am. Chem. Soc.* **2005**, *127*, 534–535.
- [10] a) T. E. O. Screen, J. R. G. Thorne, R. G. Denning, D. G. Bucknall, H. L. Anderson, *J. Am. Chem. Soc.* **2002**, *124*, 9712–9713; b) K. Ogawa, A. Ohashi, Y. Kobuke, K. Kamada, K. Ohta, *J. Am. Chem. Soc.* **2003**, *125*, 13356–13357; c) T. E. O. Screen, J. R. G. Thorne, R. G. Denning, D. G. Bucknall, H. L. Anderson, *J. Mater. Chem.* **2003**, *13*, 2796–2808; d) M. Drobizhev, Y. Stepanenko, A. Rebane, C. J. Wilson, T. E. O. Screen, H. L. Anderson, *J. Am. Chem. Soc.* **2006**, *128*, 12432–12433; e) J. E. Raymond, A. Bhaskar, T. Goodson, III, N. Makiuchi, K. Ogawa, Y. Kobuke, *J. Am. Chem. Soc.* **2008**, *130*, 17212–17213; f) S. Easwaramoorthy, S. Y. Jang, Z. S. Yoon, J. M. Lim, C.-W. Lee, C.-L. Mai, Y.-C. Liu, C. Y. Yeh, J. Vura-Weis, M. R. Wasielewski, D. Kim, *J. Phys. Chem. A* **2008**, *112*, 6563–6570.
- [11] a) T. K. Ahn, J. H. Kwon, D. Y. Kim, D. W. Cho, D. H. Jeong, S. K. Kim, M. Suzuki, S. Shimizu, A. Osuka, D. Kim, *J. Am. Chem. Soc.* **2005**, *127*, 12856–12861; b) H. Rath, J. Sankar, V. PrabhuRaja, T. K. Chandrashekhar, A. Nag, D. Goswami, *J. Am. Chem. Soc.* **2005**, *127*, 11608–11609; c) J. Arnbjerg, A. Jiménez-Banzo, M. J. Paterson, S. Nonell, J. I. Borrell, O. Christiansen, P. R. Ogilby, *J. Am. Chem. Soc.* **2007**, *129*, 5188–5199; d) Y. Tanaka, S. Saito, S. Mori, N. Aratani, H. Shinokubo, N. Shibata, Y. Higuchi, Z. S. Yoon, K. S. Kim, S. B. Noh, J. K. Park, D. Kim, A. Osuka, *Angew. Chem. Int. Ed.* **2008**, *47*, 681–684; *Angew. Chem.* **2008**, *120*, 693–696; e) J. M. Lim, Z. S. Yoon, J.-Y. Shin, K. S. Kim, M.-C. Yoon, D. Kim, *Chem. Commun.* **2009**, 261–273.
- [12] a) A. Tsuda, A. Osuka, *Science* **2001**, *293*, 79–82; b) K. Y. Kim, T. K. Ahn, J. H. Kwon, D. Kim, T. Ikeue, N. Aratani, A. Osuka, M. Shigeiwa, S. Maeda, *J. Phys. Chem. A* **2005**, *109*, 2996–2999; c) Y. Inokuma, N. Ono, H. Uno, D. Y. Kim, S. B. Noh, D. Kim, A. Osuka, *Chem. Commun.* **2005**, 3782–3784; d) T. K. Ahn, K. S. Kim, D. Y. Kim, S. B. Noh, N. Aratani, C. Ikeda, A. Osuka, D. Kim, *J. Am. Chem. Soc.* **2006**, *128*, 1700–1704; e) Y. Nakamura, S. Y. Jang, T. Tanaka, N. Aratani, J. M. Lim, K. S. Kim, D. Kim, A. Osuka, *Chem. Eur. J.* **2008**, *14*, 8279–8289.
- [13] a) T. D. Lash, T. M. Werner, M. L. Thompson, J. M. Manley, *J. Org. Chem.* **2001**, *66*, 3152–3159; b) S. Richeter, C. Jeandon, N. Kyritsakas, R. Ruppert, H. J. Callot, *J. Org. Chem.* **2003**, *68*, 9200–9208; c) H. S. Gill, M. Marmjanz, J. Santamaría, I. Finger, M. J. Scott, *Angew. Chem. Int. Ed.* **2004**, *43*, 485–490; *Angew. Chem.* **2004**, *116*, 491–496; d) O. Yamane, K. Sugiura, H. Miyasaka, K. Nakamura, T. Fujimoto, K. Nakamura, T. Kaneda, Y. Sakata, M. Yamashita, *Chem. Lett.* **2004**, *33*, 40–41; e) K. Kurotobi, K. S. Kim, S. B. Noh, D. Kim, A. Osuka, *Angew. Chem. Int. Ed.* **2006**, *45*, 3944–3947; *Angew. Chem.* **2006**, *118*, 4048–4051; f) M. Tanaka, S. Hayashi, S.

- Eu, T. Umeyama, Y. Matano, H. Imahori, *Chem. Commun.* **2007**, 2069–2071; g) N. K. S. Davis, M. Pawlicki, H. L. Anderson, *Org. Lett.* **2008**, *10*, 3945–3947; h) S. Tokuji, Y. Takahashi, H. Shinmori, H. Shinokubo, A. Osuka, *Chem. Commun.* **2009**, 1028–1030; i) N. K. S. Davis, A. L. Thompson, H. L. Anderson, *Org. Lett.* **2010**, *12*, 2124–2127; j) V. V. Diev, K. Hanson, J. D. Zimmerman, S. R. Forrest, M. E. Thompson, *Angew. Chem. Int. Ed.* **2010**, *49*, 5523–5526; *Angew. Chem.* **2010**, *122*, 5655–5658.
- [14] a) A. Herrmann, K. Müllen, *Chem. Lett.* **2006**, *35*, 978–985; b) F. O. Holtrup, G. R. J. Müller, H. Quante, S. de Feyter, F. C. de Schryver, K. Müllen, *Chem. Eur. J.* **1997**, *3*, 219–225; c) H. Quante, K. Müllen, *Angew. Chem. Int. Ed. Engl.* **1995**, *34*, 1323–1325; *Angew. Chem.* **1995**, *107*, 1487–1489; d) H. Langhals, G. Schoenmann, L. Feiler, *Tetrahedron Lett.* **1995**, *36*, 6423–6424; e) Y. Geerts, H. Quante, H. Platz, R. Mahrt, M. Hopmeier, A. Böhm, K. Müllen, *J. Mater. Chem.* **1998**, *8*, 2357–2369; f) N. G. Pschirer, C. Kohl, F. Nolde, J. Qu, K. Müllen, *Angew. Chem. Int. Ed.* **2006**, *45*, 1401–1404; *Angew. Chem.* **2006**, *118*, 1429–1432; g) Z. Yuan, S. L. Lee, L. Chen, C. Li, K. S. Mali, S. de Feyter, K. Müllen, *Chem. Eur. J.* **2013**, *19*, 11842–11846.
- [15] H. S. Cho, D. H. Jeong, S. Cho, D. Kim, Y. Matsuzaki, K. Tanaka, A. Tsuda, A. Osuka, *J. Am. Chem. Soc.* **2002**, *124*, 14642–14654.
- [16] a) C. Jiao, K.-W. Huang, Z. Guan, Q.-H. Xu, J. Wu, *Org. Lett.* **2010**, *12*, 4046–4049; b) C. Jiao, K.-W. Huang, J. Wu, *Org. Lett.* **2011**, *13*, 632–635; c) J. Luo, M. Xu, R. Li, K.-W. Huang, C. Jiang, Q. Qi, W. Zeng, J. Zhang, C. Chi, P. Wang, J. Wu, *J. Am. Chem. Soc.* **2014**, *136*, 265–272.
- [17] a) Y. Li, Z. Wang, *Org. Lett.* **2009**, *11*, 1385–1388; b) C. Jiao, K.-W. Huang, J. Luo, K. Zhang, C. Chi, J. Wu, *Org. Lett.* **2009**, *11*, 4508–4511; c) Y. Li, J. Gao, S. D. Motta, F. Negri, Z. Wang, *J. Am. Chem. Soc.* **2010**, *132*, 4208–4213; d) Z. Zeng, M. Ishida, J. L. Zafra, X. Zhu, Y. M. Sung, N. Bao, R. D. Webster, B. S. Lee, R.-W. Li, W. Zeng, Y. Li, C. Chi, J. T. L. Navarrete, J. Ding, J. Casado, D. Kim, J. Wu, *J. Am. Chem. Soc.* **2013**, *135*, 6363–6371; e) Z. Zeng, S. Lee, J. L. Zafra, M. Ishida, X. Zhu, Z. Sun, Y. Ni, R. D. Webster, R.-W. Li, J. L. López Navarrete, C. Chi, J. Ding, J. Casado, D. Kim, J. Wu, *Angew. Chem. Int. Ed.* **2013**, *52*, 8561–8564; *Angew. Chem.* **2013**, *125*, 8723–8727.
- [18] Q. Ouyang, Y.-Z. Zhu, C.-H. Zhang, K.-Q. Yan, Y.-C. Li, J.-Y. Zheng, *Org. Lett.* **2009**, *11*, 5266–5269.
- [19] a) A. Tsuda, Y. Nakamura, A. Osuka, *Chem. Commun.* **2003**, 1096–1097; b) T. Ikeda, N. Aratani, S. Easwaramoorthi, D. Kim, A. Osuka, *Org. Lett.* **2009**, *11*, 3080–3083.
- [20] J. A. Page, G. Wilkinson, *J. Am. Chem. Soc.* **1952**, *74*, 6149–6150.

Received: October 9, 2014

Published online on ■■■, 0000

FULL PAPER

 $\lambda_{\text{abs}}^{\text{max}} > 1250 \text{ nm}$
 $\epsilon_{\text{max}} > 1.3 \times 10^5 \text{ M}^{-1} \text{ cm}^{-1}$

π-Extended Porphyrins

J. Luo, S. Lee, M. Son, B. Zheng,
K.-W. Huang, Q. Qi, W. Zeng, G. Li,
D. Kim,* J. Wu*

■ ■ - ■ ■

N-Annulated Perylene-Substituted and Fused Porphyrin Dimers with Intense Near-Infrared One-Photon and Two-Photon Absorption

Fusion along an axis: Fusion of two *N*-annulated perylene units to a fused Zn-porphyrin dimer along the S_0 - S_1 electronic transition moment axis of both

has resulted in organic near-infrared dyes with very intense absorption beyond 1250 nm. They also show large two-photon absorption cross-sections.